# Geometry and electronic structure of $\alpha$-Pu: A theoretical study

Babak Sadigh, Per Söderlind, and Wilhelm G. Wolfer

*Lawrence Livermore National Laboratory, University of California, P.O. Box 808, Livermore, California 94550, USA*
(Received 31 March 2003; revised manuscript received 4 June 2003; published 3 December 2003)

The highly complex ground-state structure of Pu has been fully relaxed using first-principles forces and the obtained geometry compares very well with experimental data. *Ab initio* molecular-dynamics (MD) simulations at 300 K further confirm the stability of the relaxed structure, and reveal the nature of the vibrations in this system. In addition, magnetic ordering in $\alpha$-Pu is studied in detail, showing a strong tendency in Pu to develop magnetic moments that vary considerably in magnitude depending on the atomic position in the lattice, with an overall antiparallel alignment. These spin-polarized (SP) calculations reproduce, the experimental bulk modulus of $\alpha$-Pu. Combining the bulk modulus from the SP calculations, and the vibrational contribution to the thermal expansion from the MD simulations, we can account for the anomalous thermal expansion of $\alpha$-Pu.

The complex electronic structure of the actinide metals remains one of the challenges for condensed-matter theory.[1] In particular, the highly unusual electronic structure of Pu is responsible for one of the most complex phase diagrams of any element in the periodic system, containing six known polymorphs as a function of temperature.[2] Its ground-state ($\alpha$-Pu) is determined from experiments[3] to be a low-symmetry monoclinic structure described by a 16-atom unit cell containing distorted close-packed planes that are stacked along the [001] direction. It undergoes structural transitions[2] at about 390 K and 470 K to the orthorhombic structures $\beta$-Pu and $\gamma$-Pu, respectively, followed by another phase transition, at about 600 K, to the face-centered-cubic (fcc) $\delta$ phase. From a technological standpoint, this latter phase is the most important because it is ductile and easier to machine and form.

In the past, density-functional theory (DFT) calculations were shown to predict quite accurately the equilibrium volume and cohesive energy of $\alpha$-Pu, while failing spectacularly for the $\delta$ phase.[4,5] This suggested that the $\alpha$-Pu phase is rather well described within a one-electron band picture, while $\delta$-Pu has fundamentally different electronic structure, containing highly correlated $f$ electrons. On the other hand, recently it was proposed[6] that even the $f$ electrons in $\alpha$-Pu might be highly correlated. Since no attempt has been made yet to relax the experimental $\alpha$-Pu geometry, it is not clear whether the accuracy of the band calculations for this structure is only fortuitous.

In this Rapid Communication we describe a comprehensive DFT study, in the generalized gradient approximation (GGA), of the geometry of Pu metal in its ground state. We demonstrate that the GGA is able to predict very delicate details of the $\alpha$ structure when we allow all degrees of freedom to relax. Following the recent work by Söderlind,[7] which showed that allowing for spin/orbital polarization, DFT can very well reproduce the lattice constant and other properties of $\delta$-Pu, we also study below the degree of electron correlation in the $\alpha$ phase by allowing for spin/orbital polarization.

We have performed first-principles calculations using both the full potential linear muffin-tin orbitals (FPLMTO) and the projector augmented-wave (PAW) methods for Pu.

Most of the FPLMTO and PAW computational details can be found in our earlier work focused on $\delta$-Pu.[8] The former is an all-electron technique that accurately represents the non-spherical electronic charge density and crystal potential, with the added benefit (compared to PAW) of corrections for spin-orbit interaction and orbital polarization. The PAW method is a generalization of the Vanderbilt pseudopotential scheme and is implemented in the VASP code.[9] The FPLMTO and PAW total energies for $\alpha$-Pu were obtained using 16 and 27 special $k$ points in the integrations over the Brillouin zone, respectively. The $\alpha$-Pu structure was determined by full relaxation of the DFT forces and stresses obtained from the PAW calculations. This is indeed a formidable task that involves relaxing the volume, two axial ratios, a unit-cell angle, and atomic coordinates for 16 atoms. Also, the formation of magnetic moments, aligned parallel or antiparallel, were allowed in $\alpha$-Pu. The accuracy of the PAW technique was tested by comparing to selected FPLMTO results.

Let us first discuss the geometry of the $\alpha$-Pu structure. Each adjacent close-packed plane can be described by an 8-atom unit cell that is fully specified by three parameters $a$, $b$, and $\theta$. These parameters are the lengths of the two vectors spanning the distorted plane and the angle between these vectors, respectively. Table I quotes the experimental values for these parameters as well as the interlayer spacing specified by the parameter $c$. The planes are stacked such that in the (001) direction four inequivalent pairs of atoms, i.e., atoms (1,8), (2,7), (3,5), and (4,6) form interlayer chains.[3] Applying the PAW technique, the $\alpha$-Pu geometry was relaxed using both nonmagnetic (NM) and spin-polarized (SP) forces within GGA, and the results for the lattice parameters are shown in Table I. Note how well our DFT forces are able to reproduce the experimental data, especially the $c/a$ axial ratio. Also, structural relaxations within the NM PAW treatment increase the atomic volume by about 3% improving the agreement with experiment. Our relaxation scheme did not enforce inversion symmetry between the adjacent distorted close-packed planes. However, the inversion relation between the atomic positions was retained to within the numerical accuracy of our calculations. In Table II we present the atomic positions of the inequivalent atoms within one of the distorted close-packed planes and compare with the experimental positions. The agreement with the experimental

B. SADIGH, P. SÖDERLIND, AND W. G. WOLFER

TABLE I. Calculated and experimental (Refs. 3,16) crystal-structure parameters, atomic volumes ($V$), and bulk moduli ($B$) for $\alpha$-Pu. Fixed denotes values kept frozen and equal to experimental values. Atomic volumes are in units of Å$^3$ and bulk moduli in GPa. The magnetic calculations were performed for an antiferromagnetic alignment (see main text).

| Method | $b/a$ | $c/a$ | $\theta$ | $V$ | $B$ |
|---|---|---|---|---|---|
| PAW (AF) | 1.830 | 0.755 | 101.9° | 17.9 | 189 |
| PAW (NM) | 1.860 | 0.755 | 102.1° | 17.8 | 185 |
| PAW (AF) | Fixed | Fixed | Fixed | 18.1 | 79 |
| PAW (NM) | Fixed | Fixed | Fixed | 17.3 | 227 |
| FPLMTO (NM) | 1.769 | Fixed | Fixed | 18.8 | 144 |
| FPLMTO (AF) | Fixed | Fixed | Fixed | 20.3 | 50 |
| Experiment | 1.773 | 0.755 | 101.8° | 19.3 [a], 20.0 [b] | 55 [b], 67 [c] |

[a]Extrapolated to 0 K.
[b]Measured at 300 K.
[c]Measured at 100 K.

geometry is impressive. Note that the calculated atomic coordinates as well as the lattice parameters are clearly improved upon when SP forces are used. Later in this paper, we will describe in detail our magnetic calculations for $\alpha$-Pu.

Although PAW gives good results in general, it does underestimate the volume and overestimate the $b/a$ axial ratio somewhat, and for that reason we turned to the FPLMTO method. First, the total energy was minimized with respect to the atomic volume, keeping all structural parameters fixed at their experimental values. Second, at this volume, the total energy was again minimized, now with respect to the $b/a$ axial ratio. The results from these NM calculations are shown in Table I and the agreement with experiment is now considerably improved. The larger (and better) volume obtained from the FPLMTO technique is due to the inclusion of spin-orbit coupling which is well known to reduce the $f$ bonding[11–13] in $\alpha$-Pu. The NM FPLMTO volume is 18.8 Å$^3$, or 3% smaller than the experimental (zero temperature) volume, but if relaxation effects expand the volume (as in the PAW calculation) the result would be in even better agreement with experiment. Also, in the FPLMTO treatment, the $b/a$ axial ratio is identical to the experimental value.

We have further explored the potential-energy surface of $\alpha$-Pu by performing *ab initio* molecular-dynamics (MD) simulations of a 16-atom unit cell at 300 K with an atomic volume of 20 Å$^3$, starting from the experimental geometry. We find that vibrations in $\alpha$-Pu can be described in terms of harmonic phonons about atomic positions that are unchanged with temperature, i.e., the time-averaged positions in the MD simulation agree almost perfectly with the force-relaxed geometries (see Table II). The average mean-square displacement is about 5% of the nearest-neighbor distance. About half of all the vibrations in the $\alpha$ crystal are displacements along the interplanar chains. The two other degrees of freedom, within the distorted close-packed planes, are therefore stiffer and allow for smaller vibrational amplitudes. Another interesting piece of information obtained from the MD simulations is the temperature-induced change in pressure at 300 K ($\Delta P$), which is found to be 1.9 GPa. When divided with the experimental bulk modulus [$B = -V(dP/dV) = 55$ GPa] a volume expansion ($\Delta V$) of about 3% is obtained which in fact agrees very well with the experimental thermal expansion for $\alpha$-Pu at 300 K.

Next we explore the existence of magnetic moments in $\alpha$-Pu, first by extensive spin-polarized PAW calculations and then, for comparison, some selected FPLMTO calculations. Allowing for magnetism we find that the energy of $\alpha$-Pu for the experimental geometry is reduced by 3.7 mRy/atom and its equilibrium volume is expanded from 17.3 to 18.1 Å$^3$. The effect of spin polarization is far smaller for the relaxed geometry where the energy is only reduced by 1.5 mRy/atom and the equilibrium volume is expanded from 17.8 to 17.9 Å$^3$. In the PAW the spin moments are obtained by projecting the total spin density in a sphere of radius 1.6 Å around each site for the volume 18.1 Å$^3$ (see Table II). We find that a large spin moment of about $3.9\mu_B$, on site 8, is mainly responsible for lowering the energy in the magnetic calculations. On the other hand, the magnetization of site 1 is consistently quite small. Further inspection reveals that site 7 develops a large and antiparallel spin moment in response to

TABLE II. Columns 2 and 3 contain the calculated atomic positions $(x,y)$ using nonmagnetic (NM) and spin-polarized (SP) PAW forces. Column 4 shows the experimental (Refs. 3,16) positions in the $\alpha$ lattice. Columns 5–7 contain the spin ($\mu_s$) and orbital ($\mu_o$) moments from FPLMTO and $\mu_s$ from the PAW, for the experimental geometry at their respective equilibrium volumes. Below we only give the coordinates of the atoms in one of the two close-packed planes. The other plane is obtained via an inversion symmetry operation.

| Atom no. | $(x,y)$ (NM) | $(x,y)$ (SP) | $(x,y)$ (Expt.) | $\mu_s$ (FPLMTO) | $\mu_o$ (FPLMTO) | $\mu_s$ (PAW) |
|---|---|---|---|---|---|---|
| 1 | (0.154,0.324) | (0.160,0.333) | (0.162,0.345) | 0.5 | −0.3 | 0.7 |
| 2 | (0.167,0.744) | (0.169,0.749) | (0.168,0.767) | −2.0 | 1.6 | −1.6 |
| 3 | (0.318,0.091) | (0.326,0.101) | (0.340,0.128) | 2.1 | −1.6 | 1.8 |
| 4 | (0.472,0.654) | (0.465,0.651) | (0.457,0.657) | 2.3 | −1.7 | 2.2 |
| 5 | (0.618,0.018) | (0.618,0.017) | (0.618,0.025) | −2.1 | 1.8 | −1.9 |
| 6 | (0.630,0.434) | (0.635,0.440) | (0.653,0.473) | −2.6 | 2.1 | −2.5 |
| 7 | (0.930,0.284) | (0.928,0.300) | (0.926,0.328) | 2.6 | −1.9 | 2.6 |
| 8 | (0.891,0.874) | (0.891,0.867) | (0.894,0.869) | −3.4 | 2.7 | −3.9 |
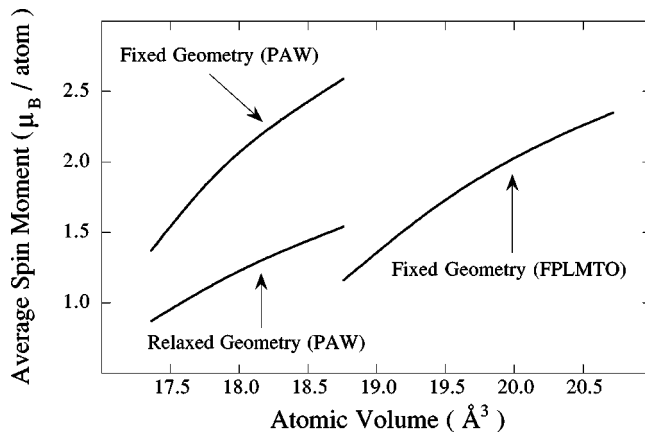
FIG. 1. Average magnitude of spin moments ($\mu_B$/atom) for $\alpha$-Pu as a function of volume ($\text{Å}^3$). "Fixed geometry" refers to results where the crystal structure has been kept fixed to the experimental parameters and "relaxed geometry" corresponds to results where the crystal structure has been allowed to relax.



FIG. 2. FPLMTO total electronic density of states for $\alpha$-Pu and $\delta$-Pu (dashed).

the large magnetization of site 8. The interlayer chains clearly play a role in determining the stable magnetic configurations of $\alpha$-Pu. In particular, we find that the sites 3 and 5, as well as 4 and 6, are paired with spin moments of similar magnitudes and opposite signs. Hence, as was previously determined for $\delta$-Pu,[7,8] and has been suggested for $\alpha$-Pu,[10] short-range antiferromagnetic (AF) ordering seems to be preferred in Pu at low temperatures.

We use the magnetic configuration above to relax the lattice parameters and the atomic coordinates of $\alpha$-Pu using the PAW forces, and we find small but clear improvement upon the NM geometry (see Tables I and II). In Fig. 1 we present the effect of structure and volume on the magnetic moments in $\alpha$-Pu by plotting the average moment per atom as a function of volume for the experimental and relaxed geometries. Note that small distortions enhance the spin moments in $\alpha$-Pu considerably. This result in conjunction with the fact that larger moments expand the atomic volume may help explain the anomalously large thermal expansion of $\alpha$-Pu. According to this theory, thermal vibrations induce distortions that increase the magnetic moments, and expand the lattice. This effect will contribute to the soft bulk modulus that is needed to account for the thermal expansion of $\alpha$-Pu. In fact for the experimental geometry, we find that the theoretical bulk modulus is considerably improved in the PAW calculations when Pu is allowed to spin polarize. Its value is reduced dramatically from $B = 227$ GPa (NM) to $B = 79$ GPA (AF), with a moderate increase in the equilibrium volume from 17.3 $\text{Å}^3$ (NM) to 18.1 $\text{Å}^3$ (AF), see Table I. For the fully relaxed structures however, the AF and NM calculations predict similar equilibrium volumes and also similar bulk moduli.

The PAW calculations lack spin-orbit interaction and therefore we chose to investigate its effect on the formation of magnetic moments using the FPLMTO formalism. As has been mentioned recently,[7] FPLMTO calculations converge to a nonmagnetic solution when ferromagnetic order is imposed. However, by introducing antiparallel alignment of the spins, spin moments ranging from about 0.4 to 3.4 $\mu_B$ (sites
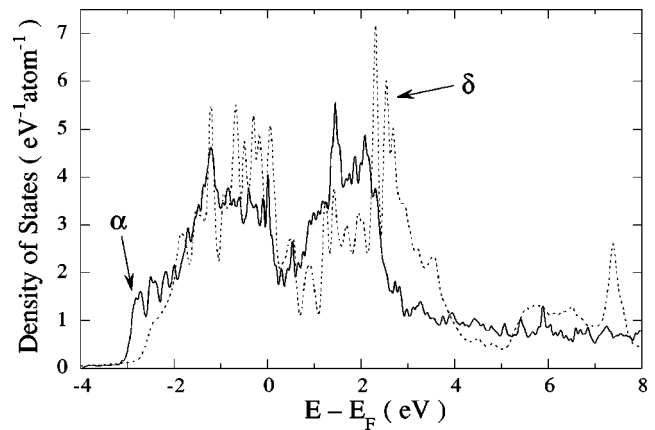
1 and 8, respectively) with antiparallel orbital moments of nearly the same magnitude are formed, which produce small total moments (0–0.7 $\mu_B$), see Table II. Figure 1 shows the magnitude of the average spin moment per atom for the FPLMTO calculations in comparison with the PAW method. Clearly the volume dependence of the FPLMTO spin moments is very similar to that of the PAW for the experimental geometry. The two curves are shifted with respect to each other, mainly due to spin-orbit coupling and orbital polarization in the FPLMTO technique. The close agreement between the two methods is further established in Table II, where the magnitudes of the FPLMTO and PAW spin moments at each site in $\alpha$-Pu are displayed.

The antiferromagnetic configuration described above lowers the total energy only slightly ($\sim 2$ mRy/atom) compared to the nonmagnetic solution. However, Table I shows that allowing for AF ordering leads to a moderate increase in the equilibrium volume and a dramatic decrease in the bulk modulus of $\alpha$-Pu, improving agreement with experiment. Compared to the NM FPLMTO calculations, the equilibrium volume increases a modest 8% whereas the bulk modulus decreases by almost a factor of three. This dramatic change in the calculated bulk modulus reflects the weaker chemical bond of the spin-polarized $5f$ orbitals, which appears to be necessary for properly describing the elastic moduli of $\alpha$-Pu. Hence combining the bulk modulus from the AF calculations with $\Delta P$ at 300 K, calculated from the *ab initio* MD simulations presented earlier in this article, we find that the anomalous thermal expansion of $\alpha$-Pu can be explained quantitatively within spin/orbital-polarized DFT. The significance of this finding is that we have thus shown that the anomalous thermal expansion of Pu is not due to anharmonic vibrations, but instead due to renormalization of the potential-energy surface when spin/orbital moments are formed.

Lastly, we show the total density of states (DOS) of $\alpha$-Pu and $\delta$-Pu as obtained from antiferromagnetic FPLMTO calculations, in Fig. 2. Note that the DOS for $\alpha$ and $\delta$ plutonium looks rather similar below the Fermi level, but $\delta$-Pu has a peak right on the Fermi level whereas $\alpha$-Pu does not. Therefore the overall photoemission spectra for $\alpha$ and $\delta$
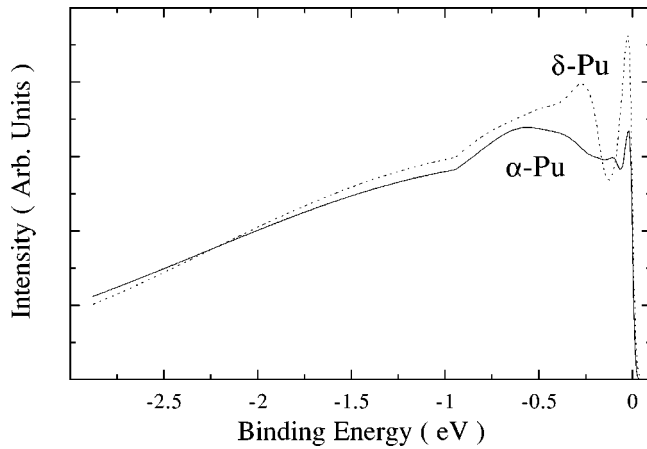
FIG. 3. FPLMTO total electronic density of states for $\alpha$-Pu and $\delta$-Pu (dashed). The spectra have been convoluted with lifetime broadening as described by Arko *et al.* (Ref. 14).

should be rather similar, although a more intense peak at the Fermi level is expected for $\delta$-Pu. To better compare with photoemission experiments, we show in Fig. 3, our calculated DOS convoluted with lifetime broadening.[14] As was pointed out[8] the DOS for $\delta$-Pu compares favorably with experiment,[14,15] but it is also clear from Figure 3, and the work by Havela *et al.*,[15] that the DOS for $\alpha$-Pu is in reasonable agreement with experiment as well. Havela *et al.*[15] showed that the strong peak in the intensity close to the Fermi level is reduced (but still present) in $\alpha$-Pu compared to $\delta$-Pu. They also showed that a weak satellite develops in $\delta$-Pu forming a valley at about $-0.3$ eV, not present in the

$\alpha$-Pu spectra. Quantitatively, this agrees well with our calculation, but the valley for $\delta$-Pu is somewhat closer to the Fermi level in the theoretical spectra. It should be mentioned that constrained local-density approximation calculations[14] are also able to reproduce the experimental spectra for $\delta$-Pu, but no other model has been shown to successfully account for the spectra of $\alpha$-Pu. In particular, it has been shown previously[14] that nonmagnetic DFT is unable to reproduce even the main features of the measured spectra of $\alpha$ or $\delta$ plutonium. From our work on $\delta$-Pu (Ref. 8) we know that the specific magnetic configuration (ferromagnetic, antiferromagnetic, or disordered) has little effect on the shape of the calculated spectra and there is no reason to expect $\alpha$-Pu to be very different in this regard.

In conclusion, we have calculated equilibrium volume, bulk modulus, and crystal-structure details of $\alpha$-Pu using PAW and FPLMTO techniques. Very extensive structural relaxations (PAW) and some selected relaxations (FPLMTO) suggest that DFT is capable of describing sensitive structural details of $\alpha$-Pu, even when the theory is constrained to the nonmagnetic limit. Formation of spin moments, however, is essential when calculating the bulk modulus which otherwise is much too high. This has implications for our understanding of the large thermal expansion in $\alpha$-Pu, which is a consequence of the very small bulk modulus and possibly also of thermally induced distortions as discussed above.

[1] S.S. Hecker, MRS Bull. **26**, 672 (2001).

[2] D.A. Young, *Phase Diagrams of the Elements* (University of California Press, Berkeley and Los Angeles, 1991).

[3] The standard enumeration of the eight inequivalent atoms in the $\alpha$-Pu structure can be found in F.W. Zachariasen and F.H. Ellinger, Acta Crystallogr. **16**, 777 (1963).

[4] P. Söderlind, O. Eriksson, B. Johansson, and J.M. Wills, Phys. Rev. B **55**, 1997 (1997).

[5] P. Söderlind and C.S. Nash, in *Advances in Plutonium Chemistry 1967–2000*, edited by D.C. Hoffman (American Nuclear Society, La Grange Park, IL, 2002), p. 6.

[6] S.Y. Savrasov, G. Kotliar, and E. Abrahams, Nature (London) **410**, 793 (2001).

[7] P. Söderlind, Europhys. Lett. **55**, 525 (2001).

[8] P. Söderlind, A. Landa, and B. Sadigh, Phys. Rev. B **66**, 205109 (2002).

[9] G. Kresse and J. Hafner, Phys. Rev. B **47**, 558 (1993); G. Kresse

and J. Furthmüller, *ibid.* **54**, 11 169 (1996); G. Kresse and D. Joubert, *ibid.* **59**, 1758 (1999).

[10] A.V. Postnikov and V.P. Antropov, Comput. Mater. Sci. **17**, 438 (2000); A.L. Kutepov and S.G. Kutepova, J. Phys.: Condens. Matter **15**, 2607 (2003).

[11] M.S.S. Brooks, J. Phys. F: Met. Phys. **13**, 103 (1983).

[12] P. Söderlind, L. Nordström, L. Yongming, and B. Johansson, Phys. Rev. B **42**, 4544 (1990).

[13] P.M. Oppeneer, T. Kraft, and M.S.S. Brooks, Phys. Rev. B **61**, 12 825 (2000).

[14] A.J. Arko, J.J. Joyce, L. Morales, J. Wills, J. Lashley, F. Wastin, and J. Rebizant, Phys. Rev. B **62**, 1773 (2000).

[15] L. Havela, T. Gouder, F. Wastin, and J. Rebizant, Phys. Rev. B **65**, 235118 (2002).

[16] H.R. Gardner, in *Plutonium Handbook*, edited by O.J. Wick Gordon (Gordon and Breach, Science Publishers Inc., New York, 1967), p. 67.